Nanoscale

An all-copper plasmonic sandwich system through directly depositing copper NPs on CVD grown graphene/copper film and its application in SERS

Journal:	*Nanoscale*
Manuscript ID:	NR-ART-02-2015-000944.R2
Article Type:	Paper
Date Submitted by the Author:	22-Apr-2015

Complete List of Authors:	li, xuanhua; Northwestern Polytechnical University, China, School of Materials Science and Engineerging; University of Hong Kong, EE Ren, Xingang; the university of hongkong, zhang, yongxing; Institute of Intelligent Machines, Chinese Academy of Sciences, Choy, Wallace; the University of Hong Kong, Electrical and Electronic Engineering Wei, Bingqing; Northwestern Polytechnical University, School of materials Science and Engineerging; University of Delaware, Mechanical Engineering

An all-copper plasmonic sandwich system through directly depositing copper NPs on CVD grown graphene/copper film and its application in SERS

Xuanhua Li,[a] Xingang Ren,[c] Yongxing Zhang,[d,*] Wallace. C. H. Choy,[c,*] Bingqing Wei,[a,b,*]

[a] State Key Laboratory of Solidification Processing, Center of Nano Energy Materials, School of Materials Science and Engineering, Northwestern Polytechnical University, Xi'an, 710072, P.R. China

[b] Department of Mechanical Engineering, University of Delaware, Newark, DE 19716, USA

[c] Department of Electrical and Electronic Engineering, the University of Hong Kong. Hong Kong , P. R. China

[d] College of Physics and Electronic Information, Huaibei Normal University, Huaibei 235000, P.R. China

*Corresponding Author: weib@udel.edu (Wei), chchoy@eee.hku.hk (Choy), zyx07157@mail.ustc.edu.cn (Zhang),

Abstract:

A simple, low-cost, all-copper sandwich system has been obtained through directly depositing Cu nanoparticles (NPs) onto a graphene sheet, which has already been grown on a Cu foil (Cu-NGF). The new design inherits two key advantages: 1)

The materials of the NGF coupling system are composed of only cheaper Cu instead of Au and Ag, 2) Direct fabrication of the system without transferring graphene will greatly lower the fabrication cost. More importantly, the Cu-NFG system shows a high sensitivity in surface-enhanced Raman scattering (SERS) with the highest enhancement factor (EF, over 1.89×10^7) reported to date in Cu plasmonic systems. Experimental and theoretical results reveal that the strong EF is mainly because of the strong near-field coupling between Cu NPs and Cu film at the optimal angle of incidence, opening up a new route for Cu materials in SERS applications.

Introduction

Surface-enhanced Raman scattering (SERS) as a powerful analytic technology has attracted successive investigations and emerging SERS substrates have been reported in the past several years.[1-6] Among various SERS substrates, nanoparticles (NPs)/gap/Film(NGF) system is of particular interest, in which metal nanoparticles (supported localized surface plasmons, LSPs) are separated from a bulk metal film (supported surface plasmon polaritons, SPPs) by a nanospacer.[7-15] Generally, the highly localized field originated by the coupling between metal NPs and a metal film is critically sensitive to the nanoscale gap.[16] However, achievement of such a reliable and precisely controlled sub-nanometer gap in an experiment is still subject to technical limitations.[17]

Graphene has attracted intense interest since its experimental discovery.[18-24] The 2-dimensional nature of graphene makes it become a favorable test bed for

investigating the SERS mechanisms.[19, 25-32] Recently, nanoantenna-sandwiched graphene with giant spectral tuning capability has been reported.[33-35] In our group, we also investigated the Ag NPs/graphene/Ag film sandwich system and achieved a strong coupling effect.[36] However, the graphene film used was grown using the chemical vapor deposition (CVD) method and should be transferred away from the grown substrate, i.e. Cu foils. The damage and/or impurities could easily be introduced into graphene during such a transfer process, which may make it difficult to investigate the optical properties of devices and explore the potential applications. In addition, the transfer process would always be time consuming, which severely hinders its future application. Therefore, constructing and studying the optical properties of a hybrid graphene–metal nanostructure without transferring the CVD grown graphene would be greatly desirable.

In addition, SERS is observed primarily on the surface of coinage metals (Au, Ag, and Cu).[37-44] Among them, a Cu substrate in SERS has its own unique advantages. For example, it is much cheaper than the other two metals, Au and Ag. In addition, Cu is particularly suitable for studying various surface phenomena in these systems using SERS techniques because of the key role in adsorption and electrocatalytic/catalytic reactions.[45-47] Unfortunately, the common Cu SERS devices show a weak SERS effect, which seriously restricts their further application. Thus, designing a suitable Cu substrate with an ultra-sensitive SERS effect is significant.

In this work, we designed and fabricated an all-Cu sandwich system through directly depositing Cu NPs onto graphene, which has already been grown on a Cu foil

(Cu-NGF, see Figure 1(a)). Two key advantages are coherently inherited in the proposed Cu-NGF coupling system: 1) all Cu materials including Cu NPs and Cu film are adopted in the coupling system, which allows a significant cost reduction of the materials compared with using noble Au and Ag metals. 2) Direct fabrication of the system without transferring graphene will also greatly reduce the fabrication time and cost. More importantly, a significant near-field enhancement between the Cu NPs and Cu film has been obtained. Especially, the highest SERS EF has been achieved with an optimal incidence angle of 60^{o} (Figure 1(b)).

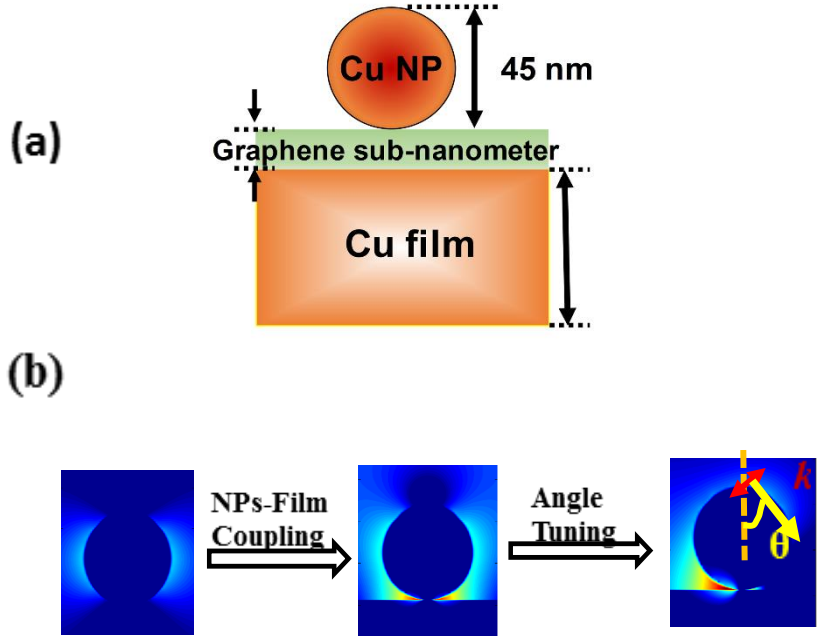

Figure 1. (a)The schematic of Cu nanoparticles/sub-nanometer graphene /Cu film (Cu-NGF) sandwich coupling system, and (b) the description about the strong near-field enhancement mainly due to the strong NPs-film coupling at an optimal incidence angle.

Experimental Section:

The Cu-NGF system fabrication

The as-proposed Cu NPs/graphene/Cu film system (Cu-NGF) was fabricated through directly evaporating Cu NPs onto the Cu film/graphene substrate with an evaporating rate of 1.0 Å/s. The CVD grown graphene was bought from Weijing Corporation in Hefei. The coverage density of Cu NPs is about 6 NPs per 100 nm^2. To fabricate Cu-NGF systems with different Cu NP coverage densities, the amount of NPs on top of Cu film can be removed through immersing the samples into acetone for different time. Acetone will easily infiltrate into the interface region between the NPs and graphene, making the Cu NPs to strip out.[36] It is found that the longer time the NPs immersed into acetone, the more the NPs were stripped out. In the current experiments, the time are 20 min and 10 min for the Cu-NFG-4NPs and Cu-NGF-2NPs samples, respectively. For the control sample Cu NPs/Graphene/Glass, it was fabricated by transferring graphene on top of a quartz glass, followed by evaporating Cu NPs onto the graphene.

Microscopic and optical characterization

The morphology of samples was characterized using scanning electron microscopy (SEM; Sirion 200). The absorption spectra of SERS substrates were extracted from the diffuse reflection (R) (1-R) using a goniometer combined with a CCD spectrometer and an integrating sphere. The sample for TEM measurement was prepared by firstly transferring a single layer graphene to copper grids and subsequently evaporating Cu NPs onto the graphene layer. Raman spectra were

obtained using a horiba HR800 Raman system with a 532 nm laser. For each sample, three SERS spectra were taken in different positions of the substrate and then averaged. To prepare the sample for copper phthalocyanine (CuPc) detection, CuPc was pre-evaporated onto the graphene for a Cu-NGF system using thermal evaporation method with evaporating rate 0.1 Å/s. The CuPc thickness was about 0.5 nm. For the sample using a silicon substrate, the thickness of CuPc is about 100 nm. The accumulated time of Raman measurement was 20 s; and laser power at the sample position was 5 mW for CuPc.

Theoretical modeling

Maxwell's equations were rigorously solved utilizing the finite-difference time-domain (FDTD) method to better understand the nature of the strong near-field enhancement in the Cu-NGF system. For simplicity, a sphere was used to study the underling physics of the proposed sandwiched system and the model structure was a 45 nm Cu NP on a 100 nm thick Cu film separated by an ultrathin monolayer graphene. The surface conductivity $\sigma(\omega)$ of an infinitesimally thin graphene sheet was calculated by the Kubo formula and the complex dielectric constant of the graphene sheet was given by the expression of $\varepsilon(\omega) = 1 - j\frac{\tilde{\sigma}(\omega)}{\omega}$, where ω is the frequency and $\tilde{\sigma}(\omega)$ is the volume conductivity of the graphene sheet, which can be obtained from the surface conductivity through the relation $\tilde{\sigma}(\omega) = \sigma(\omega)/d_0$, where d_0 is the effective thickness of the graphene sheet considered in our theoretical calculation and set as 0.5 nm.

Results and Discussion

The Cu-NGF geometry (see Figure 1) is a three-layer structure consisted of Cu NPs residing on an ultrathin graphene spacer layer grown on the Cu foil. During the fabrication process, Cu NPs are evaporated directly onto the graphene/Cu film substrate with an evaporating rate of 1.0 Å/s to form the proposed Cu-NGF system. Compared to the bare graphene/Cu film as shown in the SEM image in Figure 2(a), Cu NPs can be clearly observed on top of graphene in the Cu-NGF system (Figure 2(b)). From the TEM images as shown in Figures 2(e) and (f), quasi-sphere Cu NPs are observed. The dominant size of the Cu NPs is about 45 nm and the coverage density of Cu NPs locating on the graphene is about 6 Cu NPs per 100 nm^2 (Cu-NGF-6NPs). To fabricate Cu-NGF systems with different Cu NPs coverage, the NPs amount can be controllably removed through immersing the samples into acetone for different time. In our current experiments, the coverage density (per 100 nm^2) of another two samples including Cu-NGF with 4 NPs (Cu-NGF-4NPs, Figure 2(c)), and Cu-NGF with 2 NPs (Cu-NGF-2NPs, Figure 2(d)) can be easily obtained.

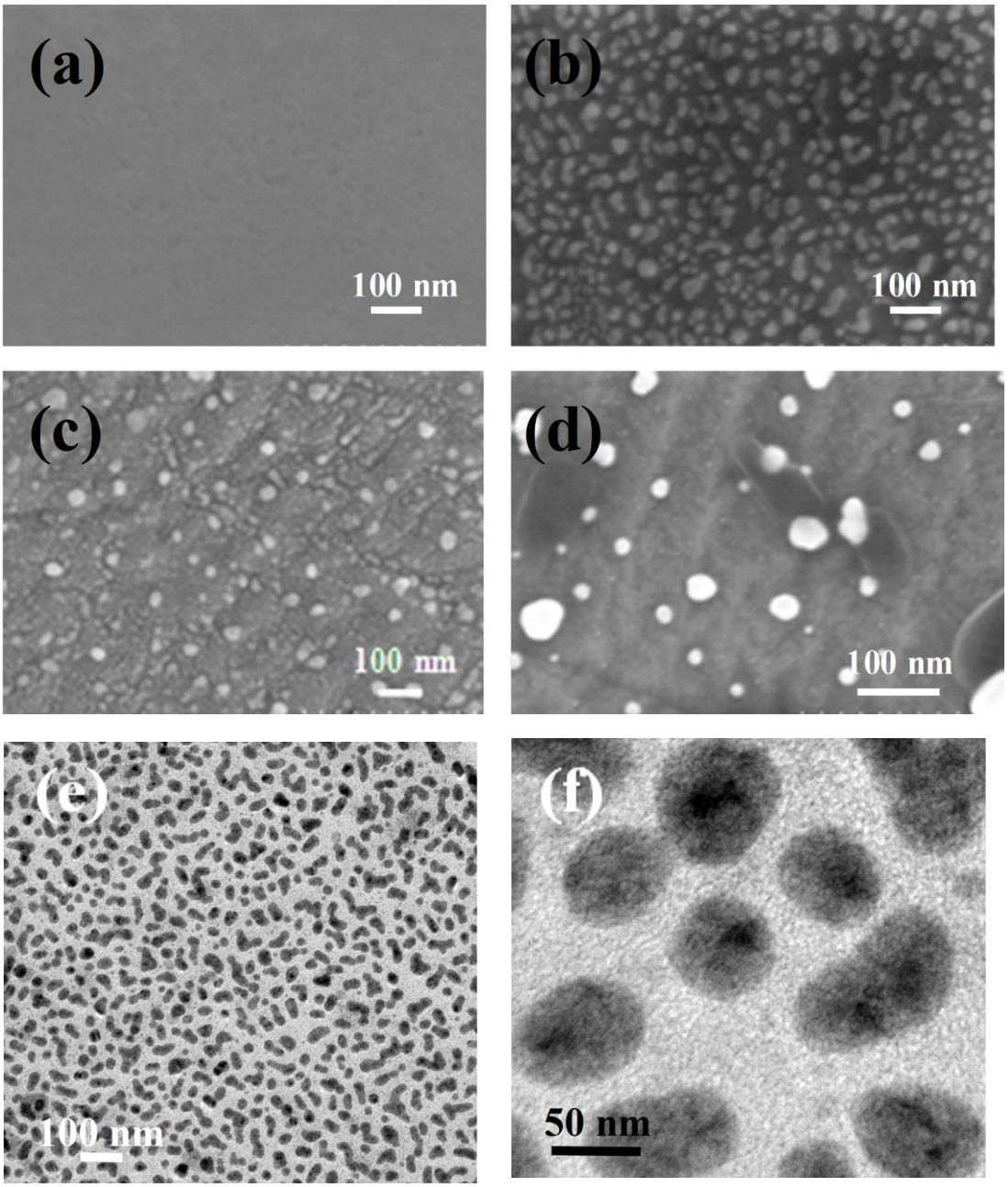

Figure 2. The SEM images of different samples: (a) bare graphene grown on Cu foil (grahene/Cu film), (b) Cu-NGF system with coverage of 6 Cu NPs per 100 nm^2 (Cu-NGF-6NPs), (c) Cu-NGF system with coverage of 4 Cu NPs per 100 nm^2 (Cu-NGF-4NPs), and (d) Cu-NGF system with coverage of 2 Cu NPs per 100 nm^2 (Cu-NGF-2NPs). (e) The TEM image and (f) high-magnified TEM image of Cu-NGF-6NPs.

The optical absorption spectra of graphene grown Cu film (graphene/Cu film), Cu NPs/Graphene/Glass, and Cu-NFG sandwich systems are investigated as shown in Figure 3. The graphene/Cu film structure shows a strong absorption edge at wavelengths shorter than 550 nm, while the Cu NPs/Graphene/Glass sample shows a strong absorption peak around 570 nm. After the Cu NPs deposition, the hybrid system presents a much stronger absorption through the entire wavelength of 350-1000 nm. As the coverage density (per 100 nm^2) of Cu NPs increases from 2 NPs (Cu-NGF-2NPs) to 6 NPs (Cu-NGF-6NPs), the absorption gradually increases and induces a broadband feature. To clearly understand the absorption enhancement, we further extract the enhancement ratio by dividing the absorption of the Cu-NFG systems with the bare graphene/ Cu film. As shown in Figure 3(b), there are two clear enhancement regions, which are around 570 nm and in the infrared region, respectively. The Cu NPs contribute to the absorption of the Cu-NFG system and lead to absorption enhancement around 570 nm, which is consistent with the plasmonic resonance of Cu NPs in previous reports.[30, 47] Moreover, this absorption around plasmonic resonanc (Figure 3(b)) becomes much stronger due to the increased coverage density of Cu NPs. In addition, another peak observed at infrared region of the sandwiched system is mainly attributed to the strong coupling between the upper Cu NPs (supported LPR) and the lower Cu film (supported SPR), with a sub-nanometer gap formed by the ultrathin graphene.[13,15,36] Interestingly, the magnitude of absorption at infrared region gradually increases when the NPs coverage density changed from 2 NPs (Cu-NGF-2NPs), 4 NPs (Cu-NGF-4NPs) to 6 NPs

(Cu-NGF-6NPs), which is mainly due to the increased amount of coupling "hot spots" between Cu NPs and copper film (denoted by the purple curve in Figure 3(b)). The coupling from Cu-NGF system with the higher coverage density of Cu NPs further strengths the localized near field between the upper Cu NPs and lower Cu film and finally leads to much strong Raman signal intensity. It is noted that the spectra shape of the second enhanced region of the sandwich structures with different particle densities seems different, which is possible due to the irregular shape of Cu NPs covering on top of graphene. In addition, the possible coupling between neighboring Cu NPs also affects the spectra shape when high-intensity Cu NPs are used in the Cu-NGF system.

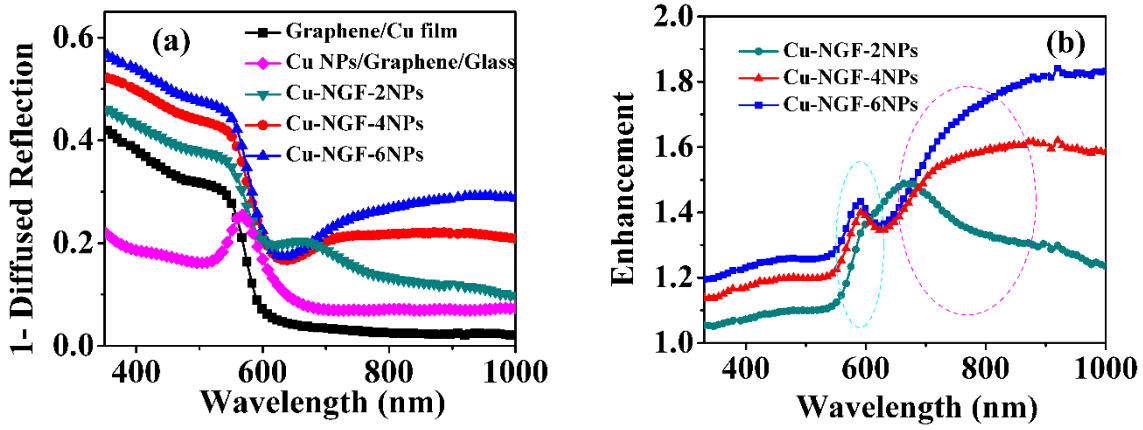

Figure 3. (a) The optical absorbance spectra of Cu-NGF sandwich coupling systems with different coverage and (b) their corresponding enhancement (for instance, (1-Diffused Reflection of sample Cu-NGF-6NPs)/ (1-Diffused Reflection of sample graphene/Cu film)).

After studying the optical absorption spectra of the Cu-NGF system, the field enhancement of Cu-NGF systems is investigated by detecting the Raman intensity

from graphene itself because the SERS intensity directly correlates with the strength of the localized near-fields that could be enhanced by the surface plasmon of Cu NPs, Cu films, and their mutual couplings.[13, 15, 36] Moreover, graphene has a well-known Raman spectrum, which could function as a favorable test bed for investigating the near-field enhancement of the G-NFG system.[27, 28] The strong coupling between the Cu NPs and Cu film will induce dramatic electromagnetic "hot spots" at the graphene sub-nanospacer, and at the same time enhance the Raman signal of graphene nearby.[35] As shown in Figure 4(a), typical Raman spectra of graphene from samples including monolayer graphene/Cu film, Cu-NGF-2NPs, Cu-NGF-4NPs, and Cu-NGF-6NPs have been investigated. Through the integration of graphene and the double Cu structures, the samples show clear Raman signals with two clear peaks. The G peak and 2D peak of graphene are around 1580cm^{-1} and 2685 cm^{-1} respectively.[26] Particularly, the intensity ratio of I(2D)/I(G)=2.8 points to the high quality and monolayer feature of the as-grown graphene (Table 1).[48] Furthermore, Raman intensity (both G and 2D peaks) of the graphene in Cu-NGF coupling system shows significant enhancement as compared to Raman spectroscopy from the graphene/Cu film, suggesting a strong coupling between Cu NPs and Cu film. We further study the enhancement ratio by dividing the SERS band intensity of graphene from Cu-NGF systems with that from the graphene/Cu film substrate (Figure 4(b)). The enhancement ratio for 2D band (G band) of monolayer graphene is 37(47), 56(78), and 73(113) for Cu-NGF-2NPs, Cu-NGF-4NPs, and Cu-NGF-6NPs, respectively. Interestingly, there is an approximately linear relation between the NPs coverage and

the enhancement ratio, which indicates that more “hot spots” between the Cu NPs and the Cu film are very beneficial for the SERS sensitivity.

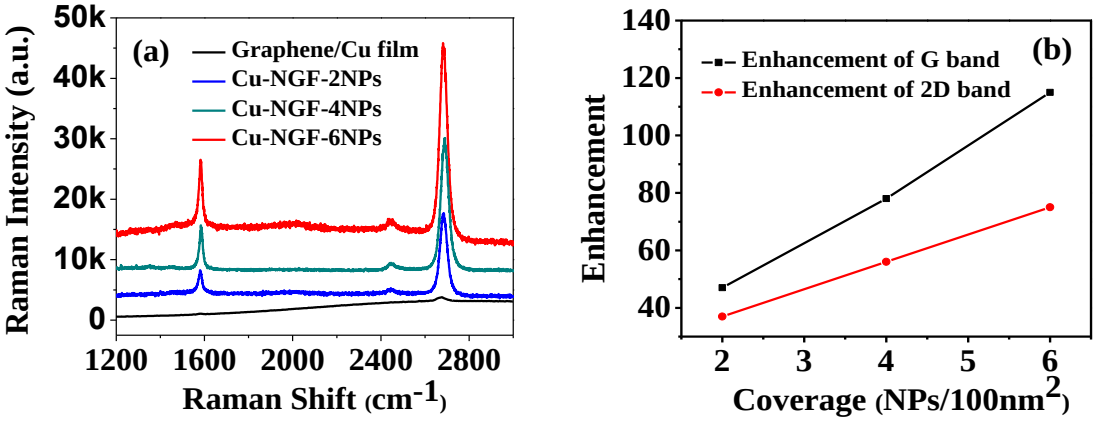

Figure 4. (a) Raman spectra of graphene enhanced by different metal nanostructures, and (b) the enhancement ratio by dividing the SERS band intensity of graphene from Cu-NGF systems with the normal Raman band intensity of the graphene grown on Cu foils. The excitation wavelength is 532 nm, the accumulated time is 10s, and the laser power is 10 mW.

Table 1. Peak information, I(2D)/I(G) and Enhancement of graphene with different samples determined from the spectra in Figure 4.

	G	2D	I(2D)/I(G)	Enhancement G band	Enhancement 2D
Graphene/Cu film	1585	2687	2.8		
Cu-NGF-2NPs	1587	2689	2.2	47	37
Cu-NGF-4NPs	1587	2690	2.0	78	56
Cu-NGF-6NPs	1588	2690	1.8	113	73

To better understand the fundamentals of the strong near-field enhancement in the G-NFG system, we rigorously solve Maxwell’s equations by utilizing the

finite-difference time-domain (FDTD) method.[49, 50] For simplicity, sphere is used to study the underling physics of the proposed sandwiched system and the theoretical structure is a 45 nm Cu NP on a 100 nm thick Cu film separated by an ultrathin monolayer graphene. As shown in Figure 5 (d), the hot spots are expected to be around the region of sub-nanospacer and the calculated EF is 6×10^4, where EF is approximately defined as the forth power of the electric field and averaged over surface 1 nm near metal nanoparticle's surface $|E_{ave}/E_0|^4$. The near field of the Cu-NGF system is very different from that of the single Cu NP, for which (Figure 5(c)) the calculated EF is just only 24, and the strong near field distributes at the two sides of Cu NP aligned with the direction of polarization and perpendicular to the incident direction of the light. As a consequence, our theoretical results reveal a greater field enhancement for the G-NFG system due to the strong coupling between Cu NPs and Cu film.

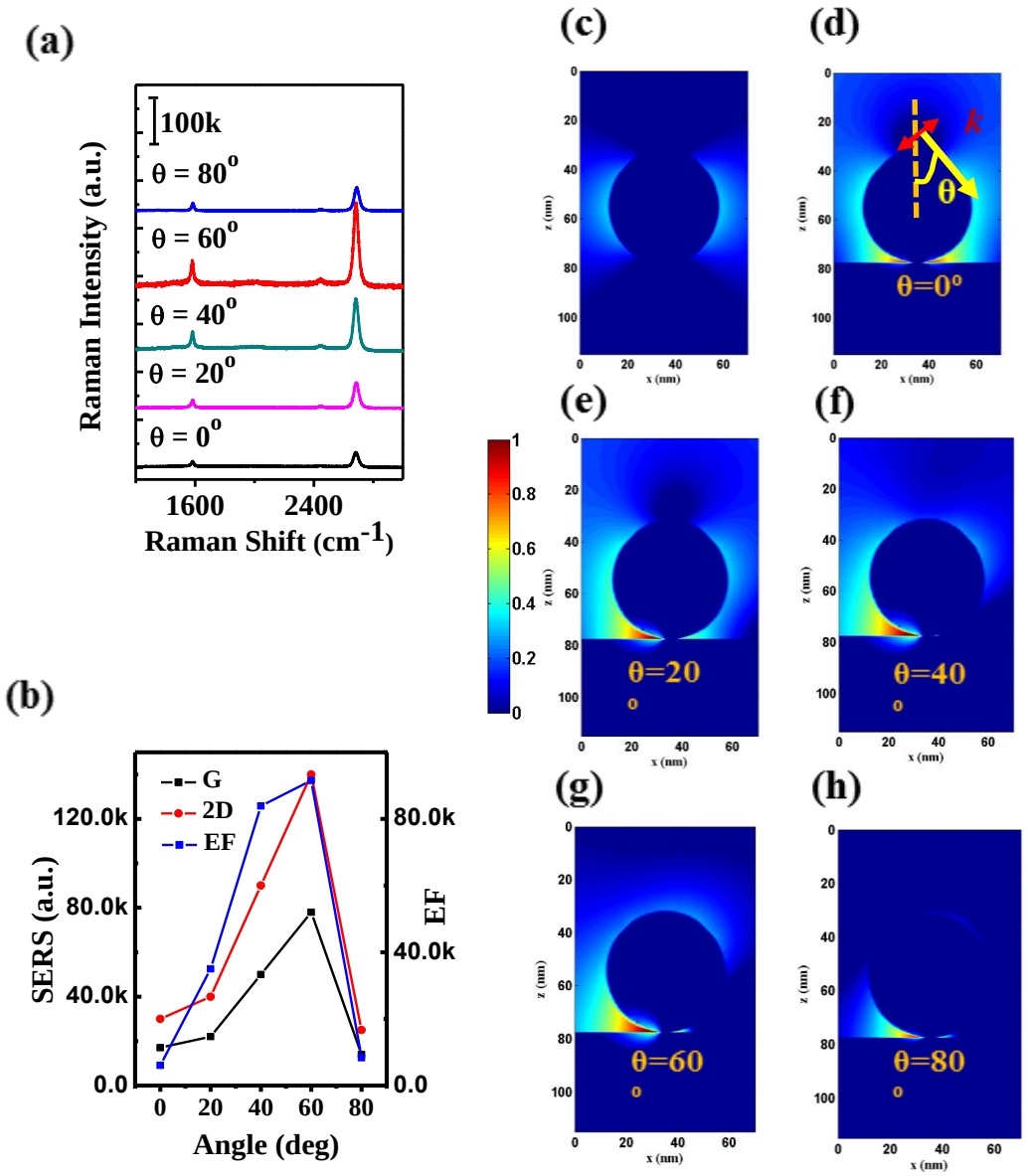

Figure 5. (a) Effect of angle of incidence on the measured SERS spectra from the Cu-NGF-6NPs, (b) SERS intensity for 2D band and G band and the calculated EF for different angle of incidence. (c) The near-filed distribution of Cu NPs, and (d)-(h) near-field distribution of Cu-NGF-6NPs at the different angle of incidence. The excitation wavelength is 532 nm.

Furthermore, the near field can be further enhanced by tuning the angle of incidence on the Cu-NGF system. Figure 5(a) shows the effect of incidence angle dependence on illuminating a Cu-NGF-6NPs system fabricated with a monolayer

graphene gap. As the incident angle varies from 0^{o}, 20^{o}, 40^{o}, 60^{o}, to 80^{o}, the Raman intensity of 2D band from graphene initially promotes from 30K, 40K, 90K, to 140K from 0^{o} to 60^{o}, respectively, and reaches a maximum value when the angle of incidence is about 60^{o}. With further increase of the incidence angle, the Raman intensity decreases to 25K. Similarly, the maximum Raman intensity of G band from graphene is obtained when the incidence angle is about 60^{o}. Interestingly, the Raman intensity of 2D(G) band at the incidence angle of 60^{o} is about 6 (5.8) times larger than that of 2D(G) band when the incidence angle is 0^{o} (Figure 5(b)). This effect is further confirmed by the theoretical near field distribution (Figure 5 (d)-(h)). When the incident angle of p-polarized light is tilted from normal angle, the normal component of electric field is increased and begins to interact with the mirror surface of the Cu film. Thus, it is possible to induce a strong coupling between Cu NPs and Cu films. The strongest coupling finally reaches the peak value at 60^{o}. However, as further increasing the incident angle, the incident and reflected light would be destructively interference due to the out of phase electric field and then reduce the normal component of the electric field. The coupling between the nanoparticle and its mirror surface will be weakened and thereby the field enhancement in the nanospacer becomes decreased. These results agree well with previous reports.[51,52] Thus, the maximum SERS sensitivity can be achieved through tilting the angle of the illuminated beam from the substrate surface normal with 60^{o} for detecting the analytes by Cu-NGF systems.

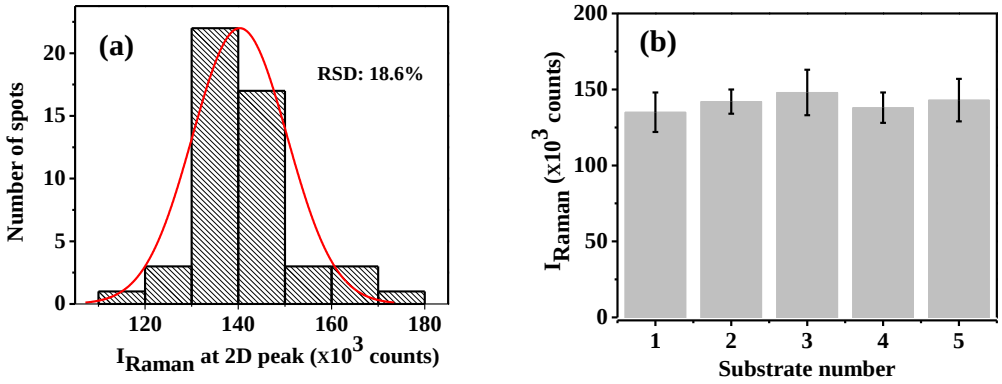

Figure 6. Examination of SERS reproducibility. (a) Spot-to-spot Raman intensity variation at 2D peak when the angle of incidence light is at 60 deg. (b) Substrate-to-substrate Raman intensity variation at 2D peak measured for five substrates.

When employing SERS technology, the reproducibility of SERS substrates should be taken into account.[42] To examine the reproducibility of the as-proposed substrate, we undertake the relative standard deviation (RSD) of the SERS signal intensity of the 2D peak at different locations to quantify the variation on one substrate (spot-to-spot variation) and between different substrates (substrate-to-substrate variation). Figure 6(a) shows the spot-to-spot variation distribution of the captured Raman intensities at the 2D peak (2687 cm^{-1}) for a randomly selected Cu-NGF-6NPs. We find that the average signal intensity for the Cu-NGF-6NPs is ca.138630 counts with a RSD of 18.6%, indicating that the Cu-NGF-6NPs has a good reproducibility across the entire area. To test the substrate-to-substrate SERS reproducibility, five Cu-NGF-6NPs substrates with the same nominal geometric parameters are loaded with CuPc of the same concentration

and a series of Raman spectra are measured at 10 different spots of each substrate to obtain an average Raman intensity. Figure 6(b) compares the substrate-to-substrate variation at the 2D peak (2687 cm^{-1}) in the Raman spectra for the five substrates, which exhibits remarkable reproducibility.

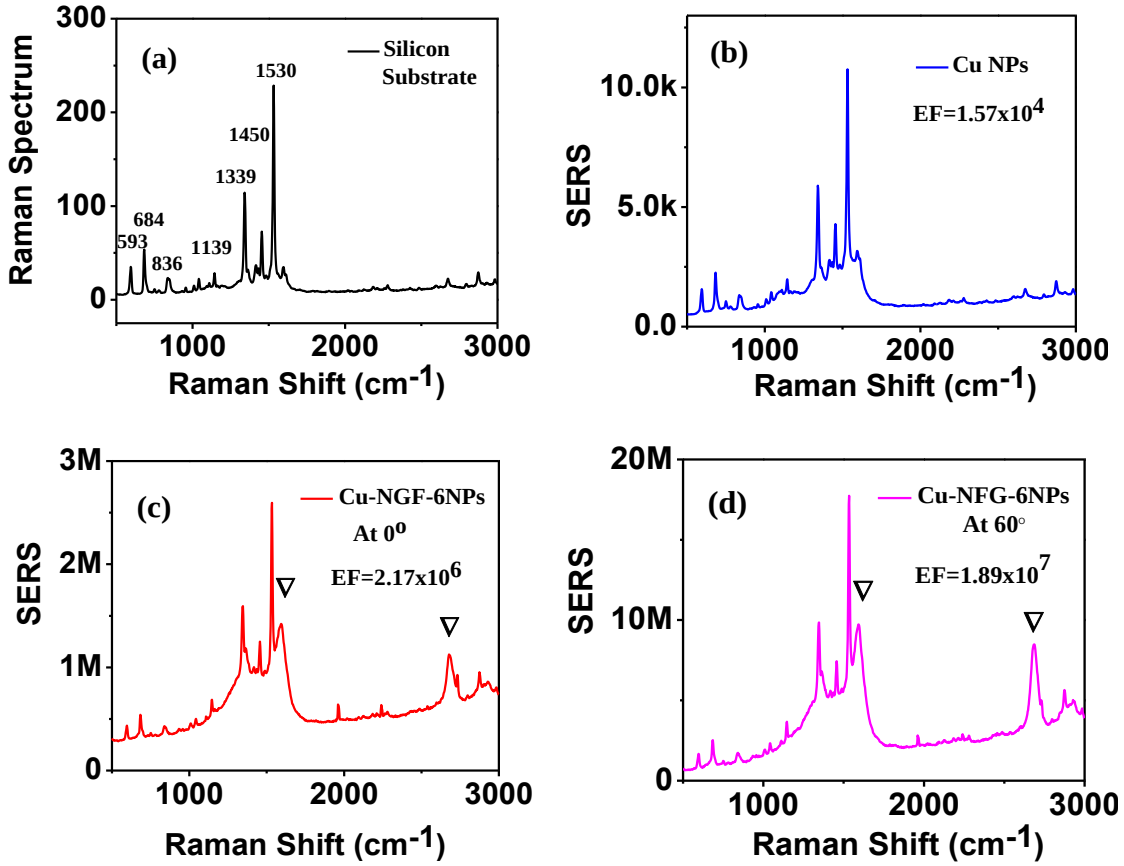

Figure 7. SERS performance of Cu-NGF-6NPs compared with that of silicon substrate and Cu NPs in detecting CuPc. "▽" denotes the Raman signals from the monolayer graphene in the Cu-NGF system. The excitation wavelength is 532 nm. The accumulated time is 20 s, and laser power is 5 mW.

Regarding the potential applications, we have investigated the sensing capability of the as-prepared Cu-NGF-6NPs system in detecting CuPc using the SERS technique. The experimental detection has been conducted at angles of incidence 0^o and 60^o. In

addition, another two samples including a silicon substrate and a Cu NPs are also used for comparison. The Cu NPs sample was obtained by depositing Cu NPs on a silicon substrate directly. The fabrication method is similar to the preparation of the Cu-NGF system and the size of Cu NPs is about 45 nm. The CuPc molecules were pre-evaporated onto graphene with 0.5 nm for Cu-NGF. For the silicon substrate sample, the thickness of CuPc is about 100 nm. Figure 7 shows the Raman spectrum of CuPc from the silicon substrate, and SERS spectra of CuPc from Cu NPs and Cu-NGF-6NPs substrates. The positions of the characteristic peaks of CuPc are generally in agreement with those reported previously.[26] For the SERS of CuPc on the Cu-NGF-6NPs substrate, we also observe the monolayer graphene Raman peak. The intensities of Raman peak at 1530 cm^{-1} on the silicon, Cu NPs and Cu-NGF-6NPs substrate at the angle of incidence of 0^o are 235, 12500, and 2560000 units, respectively, which means that the Raman signal intensity of the G-NFG substrate in detecting CuPc is 10000 times and 204 times larger compared to that of the silicon and Cu NPs substrates, respectively. More importantly, the intensity of SERS (i.e. peak at 1530 cm^{-1}) on the Cu-NGF-6NPs substrate at the incidence angle of 60^o reaches up to 18900000 units, which is nearly 80000 times and 1512 times larger compared to that of the silicon and Cu NPs substrates, respectively.

The SERS EF has been defined by $EF=(I_{SERS}/I_{bulk})\times(N_{bulk}/N_{SERS})$, where I_{SERS} and I_{bulk} are the peak intensities at 1530 cm^{-1} for the 0.5 nm CuPc on the Cu-NGF-6NPs system and 100 nm CuPc on silicon substrate, respectively , and N_{SERS} and N_{bulk} are the numbers of CuPc molecules excited by the laser beam on the Cu-NGF-6NPs and

the silicon substrate, respectively. As a result, the SERS EF is 1.57×10^4 and 2.17×10^6, for the Cu NPs and Cu-NGF-6NPs at the normal incidence (0^o), respectively. Especially, if the incident angle of an illuminated beam is set to be 60^o, the SERS EF for Cu-NGF-6NPs is increased to 1.89×10^7, which is one of the highest values reported to date in the Cu plasmonic systems. Table 2 further highlights the advantages of using the Cu-NGF system as an ultra-sensitive SERS device. The highly sensitive detection can be explained by the very strong field enhancement localized in the Cu-NFG system at the incidence angle of 60^o.

Table 2. Comparison of our work with other Cu SERS substrates reported.

Structure	Calculation method	EF	Reference
Cu/V2O5 composite	$EF=(I_{SERS}/I_{bulk})\times(N_{bulk}/N_{SERS})$ 0.01M Rhodamine 6G	1.9×10^6	Ref. 45
Cu NPs	10^{-6} M 4-mercaptobenzoic acid	/	Ref. 53
Cu nanorod arrays	$EF=\int g^4 ds/\int ds$	84	Ref. 37
Cu microcages	$EF=(I_{SERS}/I_{bulk})\times(N_{bulk}/N_{SERS})$ 10^{-7}M Rhodamine 6G	1×10^5	Ref. 38
Cu NPs/graphene oxide	10^{-8} M 4-aminothiophenol	/	Ref. 46
Cu NPs on silicon wafer	$EF=(I_{SERS}/I_{bulk})\times(N_{bulk}/N_{SERS})$ 0.01 M Rhodamine 6G	2.3×10^7	Ref. 47
CuNPs/graphene /Cu film	$EF=(I_{SERS}/I_{bulk})\times(N_{bulk}/N_{SERS})$ 0.5 nm copper phthalocyanine	1.9×10^7	**Current work**

Conclusion

In summary, we have proposed a novel, simple and low-cost all-Cu sandwich

coupling system by introducing an ultrathin monolayer graphene as a well-defined sub-nanospacer between Cu NPs and Cu films. More importantly, the Cu-NGF system is found to offer a tremendous near-field enhancement between the Cu NPs and Cu films by studying the optical absorption, Raman spectra of graphene from the Cu-NGF system, and detecting analyte CuPc. Especially, the Cu-NFG systems show a high sensitivity in SERS with the highest EF (over 1.89×10^{7}) reported to date in the Cu plasmonic systems. The strong Raman sensitivity from the Cu-NGF systems could open up a new route for Cu materials to function as a powerful tool in analytical science and the related fields.

Acknowledgments

The work is supported by the National Natural Science Foundation of China No.51472204, 51221001, and 51302102. We also thank the support from the Key Scientific and Technological Team from Shanxi Province, Start-up Funds from NWPU and Natural Science Foundation of State Key Laboratory of Solidification Processing No. 2014KA040098C040098. Choy and his team would like to acknowledge the General Research Fund (grant HKU711813), the Collaborative Research Fund (grant C7045-14E) and RGC-NSFC grant (N_HKU709/12) from the Research Grants Council of Hong Kong Special Administrative Region, China. We also thanks Dr. Di Zhang for some discussion about transfer of graphene on to a glass.

References:

1.M. P. Cecchini, V. A. Turek, J. Paget, A. A. Kornyshev and J. B. Edel, *Nature Mater.*,2013, **12**, 165-171.

2.A. Klinkova, H. Therien-Aubin, A. Ahmed, D. Nykypanchuk, R. M. Choueiri, B. Gagnon, A. Muntyanu, O. Gang, G. C. Walker and E. Kumacheva, *Nano Lett.*, 2014, **14**, 6314-6321.

3.A. Lee, G. F. Andrade, A. Ahmed, M. L. Souza, N. Coombs, E. Tumarkin, K. Liu, R. Gordon, A. G. Brolo and E. Kumacheva, *J. Am. Chem. Soc.*, 2011, **133**, 7563-7570.

4.J. H. Lee, M. H. You, G. H. Kim and J. M. Nam, *Nano Lett.*, 2014, **14**, 6217-6225.

5.M. Alba, N. Pazos-Perez, B. Vaz, P. Formentin, M. Tebbe, M. A. Correa-Duarte, P. Granero, J. Ferre-Borrull, R. Alvarez, J. Pallares, A. Fery, A. R. de Lera, L. F. Marsal and R. A. Alvarez-Puebla, *Angew. Chem. Int. Ed.*, 2013, **52**, 6459-6463.

6.X. H. Li, G. Chen, L. Yang, Z. Jin and J. Liu, *Adv. Funct. Mater.*, 2010, **20**, 2815-2824.

7.S. Mubeen, S. Zhang, N. Kim, S. Lee, S. Kramer, H. Xu and M. Moskovits, *Nano Lett.*, 2012, **12**, 2088-2094.

8.C. C. Yu, Y. C. Tseng, P. Y. Su, K. T. Lin, C. C. Shao, S. Y. Chou, Y. T. Yen and H.

L. Chen, *Nanoscale*, 2015, DOI: 10.1039/c4nr05902f.

9.C. Argyropoulos, C. Ciracì and D. R. Smith, *Appl. Phys. Lett.*, 2014, **104**, 063108.

10.H. Wei, X. Tian, D. Pan, L. Chen, Z. Jia and H. Xu, *Nano Lett.*, 2015, **15**, 560-564.

11.F. Benz, C. Tserkezis, L. O. Herrmann, B. de Nijs, A. Sanders, D. O. Sigle, L. Pukenas, S. D. Evans, J. Aizpurua and J. J. Baumberg, *Nano Lett.*, 2015, **15**, 669-674.

12.O. Daniel, M. Jan, O. H. Lars, W. B. Richard, I. Sandrine, D. Benoit, S. Yumeng, Y. Y. Hui, T. Christos, Z. Javier and J. B. Jeremy, *ACS Nano*, 2015, **9**, 825-830.

13.A. Moreau, C. Ciraci, J. J. Mock, R. T. Hill, Q. Wang, B. J. Wiley, A. Chilkoti and D. R. Smith, *Nature*, 2012, **492**, 86-89.

14. Z. Yan, Y. Bao, U. Manna, R. A. Shah and N. F. Scherer, *Nano Lett.*, 2014, **14**, 2436-2442.

15.C. Ciraci, R. T. Hill, J. J. Mock, Y. Urzhumov, A. I. Fernandez-Dominguez, S. A. Maier, J. B. Pendry, A. Chilkoti and D. R. Smith, *Science*, 2012, **337**, 1072-1074.

16. N. Yamamoto, S. Ohtani and F. J. Garcia de Abajo, *Nano Lett.*, 2011, **11**, 91-95.

17. K. J. Savage, M. M. Hawkeye, R. Esteban, A. G. Borisov, J. Aizpurua and J. J. Baumberg, *Nature*, 2012, **491**, 574-577.

18.A. C. Ferrari and D. M. Basko, *Nature Nanotech.*, 2013, **8**, 235-246.

19.S. Heeg, R. Fernandez-Garcia, A. Oikonomou, F. Schedin, R. Narula, S. A. Maier, A. Vijayaraghavan and S. Reich, *Nano Lett.*, 2013, **13**, 301-308.

20.P. Wang, O. Liang, W. Zhang, T. Schroeder and Y. H. Xie, *Adv. Mater.*, 2013, **25**, 4918-4924.

21.Y. Zhao, X. Li, Y. Du, G. Chen, Y. Qu, J. Jiang and Y. Zhu, *Nanoscale*, 2014, **6**, 11112-11120.

22.Y. Zhao, W. Zeng, Z. Tao, P. Xiong, Y. Qu and Y. Zhu, *Chem. Commun.*, 2015, **51**, 866-869.

23.X. Yu, J. Tao, Y. Shen, G. Liang, T. Liu, Y. Zhang and Q. J. Wang, *Nanoscale*, 2014, **6**, 9925-9929.

24.Y. Zhao, X. Liu, D. Y. Lei and Y. Chai, *Nanoscale*, 2014, **6**, 1311-1317.

25.P. Wang, W. Zhang, O. Liang, M. Pantoja, J. Katzer, T. Schroeder and Y. Xie, *ACS Nano*, 2012, **6**, 6244-6249.

26.W. Xu, X. Ling, J. Xiao, M. S. Dresselhaus, J. Kong, H. Xu, Z. Liu and J. Zhang, *Proc. Natl. Acad. Sci. U. S. A.*, 2012, **109**, 9281-9286.

27.Y. Du, Y. Zhao, Y. Qu, C.-H. Chen, C.-M. Chen, C.-H. Chuang and Y. Zhu, *J. Mater. Chem. C*, 2014, **2**, 4683.

28.W. Xu, J. Xiao, Y. Chen, Y. Chen, X. Ling and J. Zhang, *Adv. Mater.*, 2013, **25**, 928-933.

29. L. Zhang, C. Jiang and Z. Zhang, *Nanoscale*, 2013, **5**, 3773-3779.

30. Y. Zhao, G. Chen, Y. Du, J. Xu, S. Wu, Y. Qu and Y. Zhu, *Nanoscale*, 2014, **6**, 13754-13760.

31. X. Ling, W. Fang, Y. H. Lee, P. T. Araujo, X. Zhang, J. F. Rodriguez-Nieva, Y. Lin, J. Zhang, J. Kong and M. S. Dresselhaus, *Nano Lett.*, 2014, **14**, 3033-3040.

32. G. Sarau, B. Lahiri, P. Banzer, P. Gupta, A. Bhattacharya, F. Vollmer and S. Christiansen, *Adv. Opt. Mater.*, 2013, **1**, 151-157.

33. L. Shao, X. Wang, H. Xu, J. Wang, J.-B. Xu, L.-M. Peng and H.-Q. Lin, *Adv. Opt. Mater.*, 2014, **2**, 162-170.

34. J. Mertens, A. L. Eiden, D. O. Sigle, F. Huang, A. Lombardo, Z. Sun, R. S. Sundaram, A. Colli, C. Tserkezis, J. Aizpurua, S. Milana, A. C. Ferrari and J. J. Baumberg, *Nano Lett.*, 2013, **13**, 5033-5038.

35. D. Paria, K. Roy, H. J. Singh, S. Kumar, S. Raghavan, A. Ghosh and A. Ghosh, *Adv. Mater.*, 2015, DOI: 10.1002/adma.201404312.

36. X. Li, W. C. H. Choy, X. Ren, D. Zhang and H. Lu, *Adv. Funct. Mater.*, 2014, **24**, 3114-3122.

37. M. Keating, S. Song, G. Wei, D. Graham, Y. Chen and F. Placido, *J. Phys. Chem. C*, 2014, **118**, 4878-4884.

38. C. Kong, S. Sun, X. Zhang, X. Song and Z. Yang, *CrystEngComm*, 2013, **15**, 6136.

39. C. Lumdee, B. Yun and P. G. Kik, *ACS Photonics*, 2014, **1**, 1224-1230.

40. T. Wang, Z. Zhang, F. Liao, Q. Cai, Y. Li, S. T. Lee and M. Shao, *Sci. Rep.*, 2014, **4**, 4052.

41. A. Shiohara, J. Langer, L. Polavarapu and L. M. Liz-Marzan, *Nanoscale*, 2014, **6**, 9817-9823.

42. X. Zhang, Y. Zheng, X. Liu, W. Lu, J. Dai, D. Y. Lei and D. R. MacFarlane, *Adv. Mater.*, 2014, DOI:10.1002/adma.201404107.

43. K. Sun, G. Meng, Q. Huang, X. Zhao, C. Zhu, Z. Huang, Y. Qian, X. Wang and X. Hu, *J. Mater. Chem. C*, 2013, **1**, 5015.

44. Z.-M. Jin, W. Gu, X.-B. Shi, Z.-K. Wang, Z.-Q. Jiang and L.-S. Liao, *Adv. Opt. Mater.*, 2014, DOI:10.1002/adom.201300504.

45. Q. Cai, F. Liao, F. Hu, Y. Li, T. Wang and M. Shao, *RSC Adv.*, 2014, **4**, 6424-6429.

46. K. Zhang, *Appl. Surf. Sci.*, 2012, **258**, 7327-7329.

47. Q. Shao, R. Que, M. Shao, L. Cheng and S. T. Lee, *Adv. Funct. Mater.*, 2012, **22**, 2067-2070.

48. X. Li, J. Li, X. Zhou, Y. Ma, Z. Zheng, X. Duan and Y. Qu, *Carbon*, 2014, **66**, 713-719.

49. X. Ren, Z. Huang, X. Wu, S. Lu, H. Wang, L. Wu and S. Li, *Comput, Phys. Commun.*, 2012, **183**, 1192-1200.

50. X. Ren, W. E. I. Sha and W. C. H. Choy, *Opt. Express*, 2013, **21**, 31824-32829.

51. L. Du, D. Y. Lei, G. Yuan, H. Fang, X. Zhang, Q. Wang, D. Tang, C. Min, S. A. Maier and X. Yuan, *Sci. Rep*., 2013, **3**, 3064-3069.

52. D. Y. Lei, A. I. Fernández-Domínguez, Y. Sonnefraud, K. Appavoo, R. F. Haglund, Jr., J. B. Pendry and S. A. Maier, *ACS Nano*, 2012, **6**, 1380-1386.

53. M. Dar, S. Sampath and S. Shivashankar, *J. Mater. Chem*., 2012, **22**, 22418-22423.

Table of content

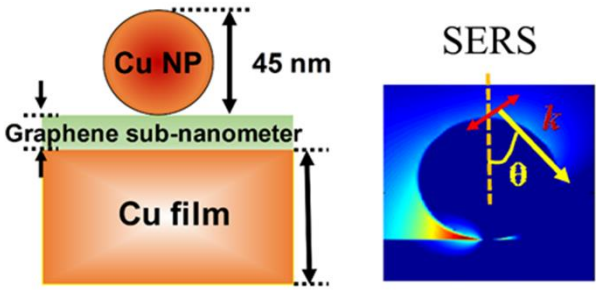

The largest SERS enhancement ((10^7) has obtained by tuning the incident angle in a simple, low-cost, all-copper sandwich system.